R. & M. No. 3136
(19,989)
A.R.C. Technical Report

R. & M. No. 3136

MINISTRY OF AVIATION

AERONAUTICAL RESEARCH COUNCIL
REPORTS AND MEMORANDA

Secondary Flow and Losses in a Compressor Cascade

By JEAN F. LOUIS

LONDON: HER MAJESTY'S STATIONERY OFFICE
1960
PRICE TEN SHILLINGS NET

Secondary Flow and Losses in a Compressor Cascade

By Jean F. Louis*

Reports and Memoranda No. 3136
March, 1958

1. *Introduction.* The shear flow on the annular walls of axial-flow turbo-machines is generally the primary cause of the difficulties encountered in the improvement of the performance and reliability of these machines. It creates a flow of lower momentum along the walls on which the pressure gradients developed in the main stream are impressed. Within a blade row, as a turning in the boundary layer equal to the turning of the free stream would not be sufficient to obtain the balance between pressure gradients and the centrifugal forces, the low-momentum fluid is turned more than the main fluid. This deviation in flow from the main stream is called the secondary flow.

The secondary flow results in the accumulation of the low-momentum flow on the suction side of the blades, and the axial symmetry is destroyed. Furthermore, in the above-mentioned accumulation area, a high loss core is often discernible. The experimental work described in this report shows that this loss core in the corner may not only be due to the secondary flow, as previously thought, but to the separation of the boundary layer in the corner formed by the junction of the wall and the blade where an important adverse gradient of pressure exists. These losses due to a stall in the corner will reduce appreciably the performance of the turbo-machines.

It is also reported that this kind of stall is associated with appreciable velocity fluctuations which could in certain cases initiate vibrations of blades such as flutter. Means of eliminating this sort of stall are discussed, and further study of the development of boundary layer in a straight corner formed by two semi-infinite planes at right angles is proposed, particularly in the case of an adverse gradient of pressure.

2. *Background and Purpose of the Set of Experiments.* The flow of fluid with non-uniform total pressure around a bend has been studied by several authors [1 to 6]. A satisfactory theory has been obtained for the flow of a non-uniform inviscid incompressible flow [1 to 5] when secondary flows are not large. More recently the behaviour of a laminar boundary layer has been studied when the free streamlines form a system of 'translates'[6]. For the cascades the problem of secondary flow appears very delicate and until now only the approach which assumes the non-uniform flow inviscid has been applied. Preston[7] assumes that in addition to the component of vorticity due to the bend of the blade passage, a change of circulation about the blade will cause circulation to be shed off into the stream. Hawthorne[8] has made further study of the different components of vorticity downstream of the cascade for small secondary flows. Hawthorne and Armstrong[9] have studied in detail the secondary-flow effects by treating the blade row as an actuator plane whose outlet angle is determined by the secondary velocities in the blade passages. Another study[10] shows that the secondary flow downstream of the cascade can be calculated from the normal vorticity and circulation distribution.

* University of Cambridge, Department of Engineering.

Agreement between the inviscid theories and the experiments is never satisfactory, as the theoretical approach does not hold near the wall where the viscous effects are strong. For compressor cascades, particularly, the magnitude of the overturning and position of the point of maximum underturning are never correctly predetermined. The high losses found in the corner between the suction side of the blades and wall have a magnitude much higher than the kinetic energy in the secondary flow. This phenomenon has been related to a local stall in that region and explained as follows: as the free-stream pressure gradients are imposed upon the boundary, the lift on the blade remains quasi-constant in that region, and as the velocity decreases towards the wall, the lift coefficient should increase rather sharply and take values which in two-dimensional flow could not be reached without stalling the cascade. The purpose of the present investigation was to find out the mechanism of the secondary flow and their associated high losses.

The first set of experiments (I, II and III) was designed to determine the effect of the large increase in lift coefficient on the losses. The experimental arrangement was similar to that used by Armstrong and Hawthorne[9] in which a wake was formed upstream of the cascade giving a spanwise velocity variation. At the centre of the wake large lift coefficients could be obtained. It was found that the losses in the region affected by three-dimensional flow were of the order of magnitude of the losses normally expected in two-dimensional flow.

The comparison was made with the secondary velocities and angle changes theoretically calculated. The experimental results showed that the secondary vorticity is apparently displaced towards the edge of the wake as a result of the widening of the wake and the consequent flattening of the velocity profile. This, of course, alters both the normal and streamwise vorticity distribution. An analysis of this effect of spreading of the wake has been successfully applied in another paper[11] to the experimental results reported here.

It was subsequently thought that the high losses found in practice could be due to the behaviour of the boundary layer in the corner between the suction side of the blade and the wall, which could separate before the two-dimensional flow. To prove this proposition, an experiment (IV) was set up in which an artificial wall was fixed at the mid-span position of the cascade. The leading edge of this artificial wall was set in the inlet plane of the cascade. As only the inlet flow was uniform, the low momentum fluid was created on the artificial wall within the cascade and its accumulation was therefore very limited. It was clearly shown that the boundary layer did separate in the corner even though the incident air angle was far from stall and the lift coefficient was small. A high loss core was recorded downstream of the cascade.

The next experiment was set up to determine the conjugate effects of the secondary flow due to a non-uniformity in entry flow and of the corner boundary layer on the artificial wall. From this set of experiments, it is concluded that the high losses near the wall of a cascade are only due to the separation of the inner boundary layer in the corner. The nature of this corner stall and its elimination are then considered. A rule for its suppression is suggested. A study of the development of a boundary layer in a straight corner formed by the intersection of two semi-infinite planes is suggested as a further step to the understanding of the behaviour of a wall boundary layer through a cascade.

3. *Apparatus, Instrumentation and Technique.* The experiments were carried out on a cascade 30 deg camber, 6 in. chord, 6 in. pitch and 18 in. span, set in the low-speed wind tunnel described in Ref. 15. In the tests, the Reynolds number based on the blade chord was kept equal to $2{\cdot}5 \times 10^5$ except when it is otherwise stated.

The non-uniformity in the inlet flow used in some experiments was the wake behind a perforated steel plate set in the mid-span plane of the cascade. The perforations in the plate make the surface rough and consequently a thick wake is obtained. The plate had the form of a parallelogram so that its leading and trailing edges were parallel to the inlet of the cascade. Its length in the streamwise direction was 18 in.

The artificial wall used in some of the experiments was made of Perspex, 0·1 in. thick. It was set up in the longitudinal plane of the cascade and extended over three passages (Photo. 3). Its leading edge was in the front plane of the cascade. Static-pressure tappings were drilled to record pressure distribution within one passage. A probe to measure yaw and total pressure was used. Atmospheric pressure was assumed to be uniform in the downstream flow.

To detect a separation zone, use was made of hydrogen sulphide which reacts with the white paint, a solution of lead carbonate in glycerin and alcohol, leaving black traces. If the hydrogen sulphide is injected into the rear of the separation region, black traces will be observed further upstream than the point of injection and will give the extent of the stall region. Photo. 1 gives an excellent view of the cascade as it was used in the last experiment (V). In the background one can distinguish the perforated steel plate; in the foreground one can see the artificial Perspex wall extending over three passages. The paint, a solution of lead carbonate, has been applied in the central section of the artificial wall and over a portion of the adjacent blade. In the right-hand corner, one can see the probe and coming from the left one observes a rubber tube which reaches one of the pressure tappings. Static-pressure tappings were also drilled around the central blade at mid-span so that the static-pressure distribution on the profile could be measured.

4. *Calculation Procedure.* For each measurement, a local coefficient giving the ratio $(P_\infty - P)/(\frac{1}{2}\rho V_{1\infty}{}^2)$ of the decrement in total head relative to the main flow to the inlet dynamic head was computed. This computation enabled the maps of the total head to be drawn.

Following cascade practice, an area-averaged loss coefficient or more exactly a decrement coefficient over a pitch length

$$\zeta = \frac{\int_0^s (P_\infty - P)\, ds}{\frac{1}{2}\rho V_{1\infty}{}^2 s}$$

was computed. As in a three-dimensional flow, continuity is not necessarily satisfied along a pitch, a mass-averaged loss coefficient or decrement coefficient may be preferred and was also computed.

$$\xi = \frac{\int_0^s \rho V \cos\alpha (P_\infty - P)\, ds}{\frac{1}{2}\rho V_{1\infty}{}^3 \cos\alpha\, s}$$

It must be noted that for experiments with a wake a decrement coefficient may also be computed for upstream conditions.

5. *Experiment I.* Experiment I was set up to determine the mechanism of the secondary flow in a cascade. The low-momentum flow involved in the secondary flow originates from the wake of the perforated plate. The cascade was set up at its nominal incidence angle, inlet angle of 55 deg. The inlet conditions to the cascade are presented in Fig. 1; air inlet conditions were satisfactorily uniform in the central part of the cascade but deteriorated appreciably towards blade ends.

Fig. 2 and Fig. 3 give the decrement in total-head contours $(P_\infty - P_2)/(\frac{1}{2}\rho V_{1\infty}{}^2)$ behind the blades. The contours cover blade pitch from the mid-span plane of symmetry of the cascade wall. The rotation of the planes of equal total pressure between the two planes of measurements (2 in.

downstream and 6 in. downstream) is quite noticeable. Fig. 4 shows the loss contours in the incident wake and the ideal loss contours on which later predictions will be based. The secondary vorticity in the streamwise direction (ξ) was calculated from the formula given in Ref. 10:

$$\xi = \frac{1}{\cos \alpha_1 \quad \cos \alpha_2} \left[\frac{\sin 2\alpha_2 - \sin 2\alpha_1}{2} + \alpha_2 - \alpha_1 \right]$$

From this secondary vorticity, the secondary velocities may be calculated downstream of the cascade. On the other hand, the time for a particle passing from upstream to downstream may be calculated from the potential flow, and therefore the displacement of particles due to secondary motion may be approximated and the lines of equal total pressure may be drawn. From the secondary velocities, outlet air angles may be predicted. These results based on an inviscid-fluid theory are compared in Figs. 4 and 5 with experimental results. It may be noted in Fig. 4 that the wake has actually spread towards the main flow, due to a spanwise redistribution of the vorticity resulting from a flattening of the velocity profile. The latter viscous effect on streamwise vorticity has been investigated theoretically in Ref. 11 and a prediction according to this theory is given in Fig. 5; agreement with experiments is good. This rotational-flow theory could for other experiments predict more exactly the spanwise position of the point of maximum underturning.

Losses. Three-dimensional or secondary flows have long been thought to cause losses, particularly in this case where the lift coefficient is high (*i.e.*, towards the mid-span plane of the wake in these experiments). A first computation of the results of the Test 1 gives the variation of

$$\zeta = \frac{\int_0^s (P_\infty - P_1)\, ds}{\frac{1}{2}\rho V_{1\infty}{}^2 s}$$

for the inlet flow along the span of the blade. This curve can be compared in Fig. 6 with similar curves obtained by computation of the results for the traversing planes respectively 2 in. and 6 in. downstream of the cascade. Similarly ξ_1 and ξ_2 were computed for the inlet flow and the traversing plane 2 in. downstream; the results are plotted in Fig. 7.

The integrated difference between the two full lines of Fig. 7 gives the losses over the area between the plane of symmetry and the region where the flow is two-dimensional. The integrated loss is within 10 per cent of the loss that one would expect if a flow with the same inlet dynamic head was kept two-dimensional. The losses associated with the latter flow are given by the area under the dotted line in Fig. 7. If the kinetic energy of the secondary flow were not recovered, it would account for a loss of about 83 per cent of the two-dimensional loss as calculated according to Ref. 10.

The static-pressure distribution around the blade in the central part of the wake may be compared with the corresponding pressure distribution for a two-dimensional flow (Fig. 16). It can be seen that the pressure gradient on the upper surface of the blade is slightly less when the flow is three-dimensional, *i.e.*, in the wake.

The lift coefficients based on the main-flow dynamic head were: for a two-dimensional flow, $C_{L\infty} = 0{\cdot}759$ and for test I at mid-span position, $C_{L\infty} = 0{\cdot}630$. The lift coefficient for test I in the mid-span plane based on the inlet dynamic head in the same z plane is $C_L = 1{\cdot}015$.

Conclusion. Although the latter lift coefficient is high, the total pressure loss through the cascade is of the order of magnitude of the two-dimensional loss. The three-dimensional loss is therefore small and is even a fraction of the kinetic energy in the secondary flow. The behaviour of secondary

flow on the cascade walls is completely different (Figs. 2 and 3). A high loss core and important rotation of the planes of equal total pressure between the two planes of measurements 2 in. and 6 in. downstream may be observed.

6. *Experiment II.* A more severe test to find out the mechanism of the end losses in a cascade was devised by performing an experiment similar to Experiment I but at the incidence for which the cascade stalls in two-dimensional flow. Fig. 8 is a map of the total-head distribution in the traversing plane 6 in. downstream of the cascade and on one side of the plane of symmetry of the wake. In the central region affected by the wake, the lines of equal total head are appreciably skewed. Fig. 11 shows the large angle variations at mid-pitch along a half-span which can be expected by theory.

Losses. The coefficients ζ and ξ were computed and their variation in the spanwise direction is presented in Fig. 9. Again it appears that three-dimensional or secondary flow does not involve large losses but may even take place with reduced losses. This can be assessed by integrating the area under the ξ curve for upstream and downstream conditions and comparing the difference of these areas extending over 2·5 in. in the spanwise direction with a predicted loss based on the coefficient ζ or ξ. But this procedure is not very rigorous as the flow is nowhere two-dimensional because of the large contraction effects taking place.

The static-pressure distribution around the blade in the plane of symmetry of the cascade was recorded for the two-dimensional flow and for the test II. These results are plotted in Figs. 12 and 13; they show that the lift varies little and that the separation region corresponding to the portion of the curve for which the static pressure is constant is smaller in a three-dimensional flow. It can also be seen that the discontinuity in static pressure associated with a laminar separation (Fig. 13) does not exist in the three-dimensional flow.

Although the incidence was much higher in this experiment and the blade stalled in a large region adjacent to the wall, the conclusions reached are the same as for Experiment I, *i.e.*, the order of magnitude of the losses remain the same in a three-dimensional flow even if the lift coefficient based on the local inlet velocity is very high.

7. *Test III.* More severe inlet conditions could be realised by having an inlet wake with a sharper velocity gradient and a much smaller minimum velocity. These conditions were difficult to obtain and when reached, appreciable variations in inlet air angles were recorded. Nevertheless, this experiment allowed the same qualitative conclusion that no important losses are associated with an isolated secondary flow. This experiment is not reported as it does not shed any new light and as the inlet conditions were far from uniform.

8. *Test IV.—Nature of the Losses near the End Walls.* None of the three previous experiments has shown any appreciable losses associated with isolated secondary flow or a stall due to a high lift coefficient in the part of the blade immersed in the wake but, on the other hand, high losses are reported on the end walls at the intersection with the suction side of the blades. The influence of a wall on the secondary flow and the losses must be studied. As the boundary layer growing at the intersection of the wall and the suction side of the blades develops in an adverse gradient of pressure and is subject to a concentration of viscous effects due to the corner, it would be thought that this corner boundary layer might separate much earlier than the two-dimensional boundary layer.

To prove this proposition, a simple experiment was devised: a thin Perspex wall was set up in the mid-span plane of the cascade such that its inlet leading edge coincided with the inlet plane of the cascade. As the inlet airflow was kept uniform, low-momentum fluid was created only within the cascade by shear effects and was therefore very small.

The map of the downstream loss contours is given in Fig. 14; high losses were recorded and a certain clockwise rotation of the fluid seems to have taken place. The high loss was found to result from a separation region existing in the corner and having its origin at about 2 in. from the trailing edge of the blades. Three proofs of this separation were collected:

(*a*) The static-pressure distribution around the blade in the plane of symmetry of the cascade (Fig. 16) shows that a considerable adverse pressure gradient exists on the suction side of the blade and precedes a region of constant pressure, generally associated with separation.

(*b*) The static pressure-distribution on the wall within one blade passage shows a separation region that the isobars circumscribe, instead of meeting the blade surface normally (Fig. 17).

(*c*) An investigation was carried out with hydrogen sulphide. The wall and a part of the blade were covered with a white paint of lead carbonate dissolved in glycerin and alcohol. The hydrogen sulphide was introduced near the trailing edge and through a pressure tapping marked with a needle on Photo. 2. The latter shows clearly that the black trace of hydrogen sulphide has moved towards the leading edge in the corner region. This indicates separation over an area of which the extent agrees consistently with the separated region determined on Fig. 17.

The same experiment was reproduced at a much lower flow: $Re = 0{\cdot}7 \times 10^5$ and a larger separation was recorded (Photo. 3).

The loss coefficients ζ and ξ were computed and plotted against the span in Fig. 15. The integrated loss over the area between the wall and the spanwise position marked 3 in. is about 194 per cent of the corresponding loss for a two-dimensional flow over the same area. Outlet air angles at mid-pitch are given in Fig. 23; which suggests that small secondry flows took place in this experiment.

Conclusion. This experiment suggests that the end-wall losses result primarily in a separation of the boundary layer in the corner formed by the end wall and the suction side of the blade. This dismisses the argument that early stall is due to a high local lift coefficient; the local C_L was equal to $0{\cdot}653$ in this experiment.

9. *Experiment V.* In the previous experiments, mainly I and IV, the independent effects of the quasi-inviscid rotational flow and of the shear flow have been examined separately. Experiment V is the synthesis of the two effects; the inlet conditions were kept the same as for Experiment I, but the cascade was divided in two parts by the Perspex wall as in IV.

The total-head contours measured near the junction of the wall and the blade (Fig. 14) show a core of losses which on the suction side of the blade is roughly equivalent to the core measured in Experiment IV. Outside that core, the effects of secondary flow caused by the upstream non-uniform velocity profile are seen and may be compared with similar effects recorded in Experiment I and plotted in Fig. 22. Evidence was collected to show that in this case again, the high-losses core resulted from a separation of the corner boundary layer on the suction side of the blade, *viz.*,

(*a*) The static-pressure distribution around the blade given in Fig. 16, shows that both the gradient of pressure on the convex side of the blades and the separation region are slightly smaller.

(*b*) The static-pressure distribution (Fig. 20) on the wall, within one blade passage shows a separation near the trailing edge of the blade.

(*c*) The investigation with the hydrogen sulphide (Photos. 4 and 5) shows again the existence of backward flow in the corner, but the trace is more widely spread over the blade surface than in Experiment IV, as an effect resulting from the much stronger secondary flow.

The two coefficients ζ and ξ, were computed at different span-wise positions and plotted on Fig. 21. The variation of air outlet angle at mid-pitch (Fig. 23) indicates large deflections near the wall, much greater than for test I (Fig. 5) and test V (Fig. 23). The distance from the wall of the maximum underturning seems to be roughly the same for Experiments I and V. It appears that the stall in the corner did not affect appreciably the position of underturning, neither did the effect of diffusion of vorticity accounted by the theory of Ref. 11. This experiment proves that the upstream non-uniform velocity profile originating the secondary flow has little effect on the losses due to the corner stall. The latter seems to be only determined by the development of the inner boundary layer.

10. *Conclusions.* 1. It is proved that high end losses are due only to the separation of the boundary layer in the corner formed by the wall and the convex surface of the blades.

2. The argument that the early stall at the ends of the blades is due to the high local lift coefficient where the blade is immersed in the end-wall boundary layer is dismissed as it is shown in the following Table for experiments with $\alpha_1 = 55$ deg.

Experiment	Conditions in the plane of symmetry	$C_{L\infty}$	C_L
Two-dimensional flow	No separation	0·759	0·759
I	No separation	0·630	1·015
IV	Separation	0·653	0·653
V	Separation	0·565	0·892

3. It is established that rotational flow or secondary flow isolated from any shear-flow effect involves losses of the same order of magnitude as for the two-dimensional flow.

4. The maximum underturning is quite smooth and therefore it is difficult to define its position and the factors which influence the latter. It is nevertheless believed that its position must be generally affected by the importance of the corner stall and the effect of the diffusion of vorticity (Ref. 11).

5. The effect of the diffusion of vorticity towards the main flow found in Experiment I was explained by the theory of Ref. 11. A further step to calculate approximately the secondary flow in the presence of a wall would be to calculate the velocity profile at the edge of the boundary layer (by the theory of Ref. 11) and match this with a velocity profile calculated by an approach similar to Ref. 6, in such a way that the momentum equations are satisfied.

11. *Nature, Possible Effects of the Corner Stall and Recommendations for its Elimination.* As might be expected, the corner stall emphasized in the previous Section has been found at first at the juncture of the wing and the fuselage of aeroplanes. Two interesting reports deal with this problem; the first sheds some light on the nature of the stall and the second on its elimination.

(*a*) Krzywoblocki in a brief review on buffeting (Ref. 12) reports that the latter is mainly caused by disturbances arising at the juncture of the wing and fuselage. These disturbances arise even for small angles of attack and usually in an asymmetrical manner.

(*b*) Hovgard reports (Ref. 13) that a remedy for that type of stall was the use of expanding fillets at the juncture, or of blisters which increase the camber of the wing. By these means higher maximum-lift coefficients were attained and stall was delayed.

These reports suggest that the corner stall may in certain cases cause such phenomena as flutter and that fillets may eliminate it and therefore limit the loss. This unsteady-flow character of the corner stall was shown in an experiment on a small compressor cascade with span to chord ratio equal to 10. The blades were 30 deg camber, 1·56 in. chord, 1 in. pitch and 25 deg stagger. The Reynolds number for the first test was $0{\cdot}9 \times 10^5$ and the inlet angle was 40 deg, which corresponds to zero incidence. A hot wire was used in the investigation; its signal after amplification went either to an oscilloscope or to a tuned amplifier so that it could be eventually analysed. The hot wire placed either in the wake of blades immersed in the main stream (Photo. 6, upper signal) or near the wall at mid-pitch (Photo. 7, upper signal). The signals show the turbulence of the flow which is rather small. When the hot wire is placed in the corner formed by the suction side of the blade and the side wall, large fluctuations are registered (Photo. 7). The response of the tuned amplifier which was tuned at 100 c.p.s. (lower signal of 6, 7, 8), is much higher than in the two other cases and is largely modulated in amplitude. The latter shows a certain similarity with certain oscillograms of flutter.

The corner stall may therefore originate vibrations of blades. For example, Khalil[14] reports the failures occurring at the root and tip of the diaphragm blades of a steam turbine. After a careful study of all the possible causes for this failure, the author suggests that it may be due to the passage vortex associated with secondary flow. As the latter vortex is steady, it seems to be more plausible to suggest that the failure of these thin blades of very long chord were caused by the corner stall which induced local vibration.

Elimination of the Corner Stall. It has been suggested in the previous paragraph that the corner stall at the juncture of the wing and fuselage could be eliminated by an expanding fillet.

This method is already applied in axial-flow compressors by some manufacturers who build axial-flow compressors having low blade loading ($\cos \alpha_1/\cos \alpha_2 \geqslant 0{\cdot}7$) at high stagger. On the other hand, designers of turbines or compressors having high blade loading limit the fillets to the minimum size required by stress analysis. If one realizes that the contraction ratio (as defined in Ref. 15), gives an order of magnitude of the end effects in a cascade, the answer to the above mentioned question seems to be suggested by the conclusion of the investigation carried out by H. G. Rhoden[15] on cascades of span/chord ratio equal to 3, with no fillets. The experiment was carried out for different cascades of blades having different cambers but the same air outlet angle and the same pitch/chord ratio. It is reported that large values of contraction are associated with large air deflections but the contraction is not greater than 10 per cent until deflections exceed 20 deg.

This seems to explain the practice of some manufacturers that low air-deflections corner stall may be avoided by fillets, but the same practice cannot eliminate this effect for large air deflections.

Until further evidence has been found, it seems reasonable to suggest that expanding fillets between the wall and the suction side of the blades could be used as a means of reducing losses as long as the design loading is kept below the limitations given by the different authors. For higher loading or deflection, boundary-layer control such as suction of the corner boundary layer should be used for reducing losses.

Further Research. The nature of the end losses, and some means of suppressing them, seem to be known but the exact behaviour of the boundary layer through the cascade and the magnitude of the eventual losses are not known. As the secondary-flow theories, based largely on the assumption that the fluid is inviscid, seem to apply reasonably well to the outer part of the layer, it seems also that the general behaviour of the whole boundary layer could be well explained if the important and localised viscous effects could be superimposed on the secondary flow.

It was therefore thought that the flow in a straight corner formed by two semi-infinite planes should be studied in two cases: (i) with no external gradient of pressure and (ii) with an adverse gradient of pressure. This study should first determine the amount of vorticity associated with a corner boundary layer and secondly give the loss coefficients associated with the corner stall.

12. *Conclusions.* 1. It has been shown that a rotational flow through a cascade isolated from any wall effect can be predicted by the theory of Ref. 11 and does not produce losses higher than for a similar two-dimensional flow.

2. Once a wall is introduced, a core of losses appears at the intersection of the wall and the suction side of the blade and results from a local stall associated with large velocity fluctuations. The core of losses seems to be independent of the intensity of the secondary flow.

3. For a better understanding of the behaviour of a wall boundary layer through a cascade it is proposed to study the development of a boundary layer in a straight corner with and without an adverse-gradient pressure.

NOTATION

P_∞	Free-stream total pressure
$P_\infty - P_1$	Upstream decrement in total head
$P_\infty - P_2$	Downstream decrement in total head
$V_{1\infty}$	Free-stream inlet velocity
α_1	Inlet air angle
α_2	Local outlet air angle
s	Pitch length
ρ	Air density
P	Local total pressure
V	Local air velocity
ζ	Mean area loss or decrement in total-pressure coefficient
ξ	Mean mass loss or decrement in total-pressure coefficient
$C_{L\infty}$	Lift coefficient based on the inlet main-stream dynamic head
C_L	Lift coefficient based on the inlet dynamic head in the plane of symmetry of the cascade

REFERENCES

No.	Author	Title, etc.
1	W. R. Hawthorne	Secondary circulation in fluid flow. *Proc. Roy. Soc.* A.206. 374. 1951.
2	H. B. Squire and K. G. Winter ..	The secondary flow in a cascade of aerofoils in a non-uniform stream. *J. Ae. Sci.* 18. 271. 1951.
3	R. E. Kronauer	Secondary flow in fluid dynamics. Proc. 1st U.S. National Congress of Appl. Mech. 747 to 56. 1952.
4	H. Eichenberger	Secondary flow within a bend. *J. Math. Phy.* 32. 34. 1953.
5	W. R. Hawthorne	The secondary flow about struts and aerofoils. *J. Ae. Sci.* 21. 588. 1954.
6	H. Z. Herzig and A. G. Hansen ..	Experimental and analytical investigation of secondary flows in ducts. *J. Ae. Sci.* 24. 217. 1957.
7	J. H. Preston	A simple approach to the theory of secondary flows. *Aero. Quart.* 5. 218. 1954.
8	W. R. Hawthorne	Rotational flow through cascades. Part I.—The components of vorticity. *Quart. J. Mech. App. Math.* 8. 266. 1955.
9	W. R. Hawthorne and W. D. Armstrong	Shear flow through a cascade. *Aero. Quart.* VII. 247. 1956.
10	J. F. Louis	Rotational inviscid flow through a cascade of blades. Ph.D. Thesis. Cambridge University. 1957.
11	J. F. Louis	Rotational viscous flow. International Congress of Applied Mechanics. Communication I. 244. 1956.
12	M. Z. Krzywoblocki	Investigation of the wing wake frequency with application of the Strouhal number. *J. Ae. Sci.* 12. 51. 1945.
13	P. E. Hovgard	Means of suppression of interference burble. *J. Ae. Sci.* 7. 1940.
14	K. H. Khalil	Conditions of failure in some turbine diaphragm blades. *The Engineer.* 1956.
15	H. G. Rhoden	Effects of Reynolds number on the flow of air through a cascade of compressor blades. R. & M. 2919. June, 1952.

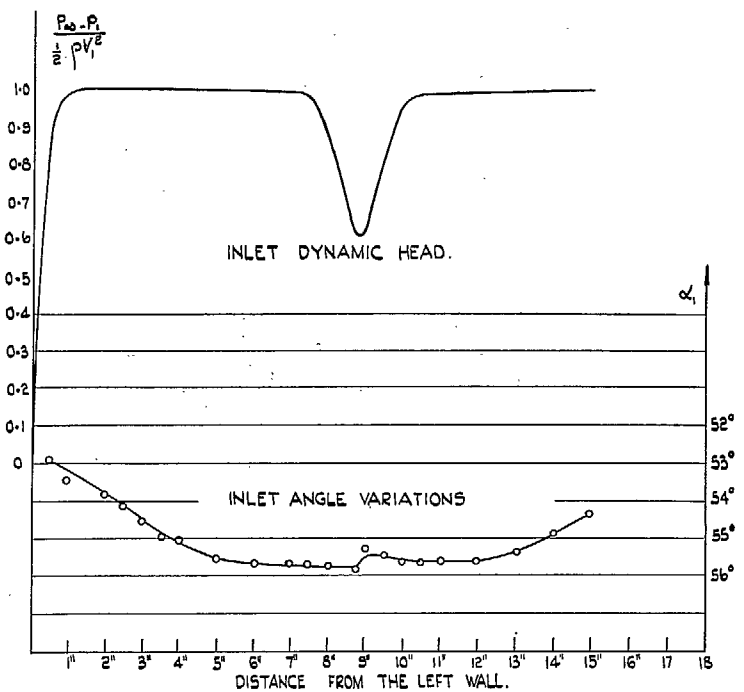

FIG. 1. Inlet conditions: $\alpha_1 = 55$ deg.

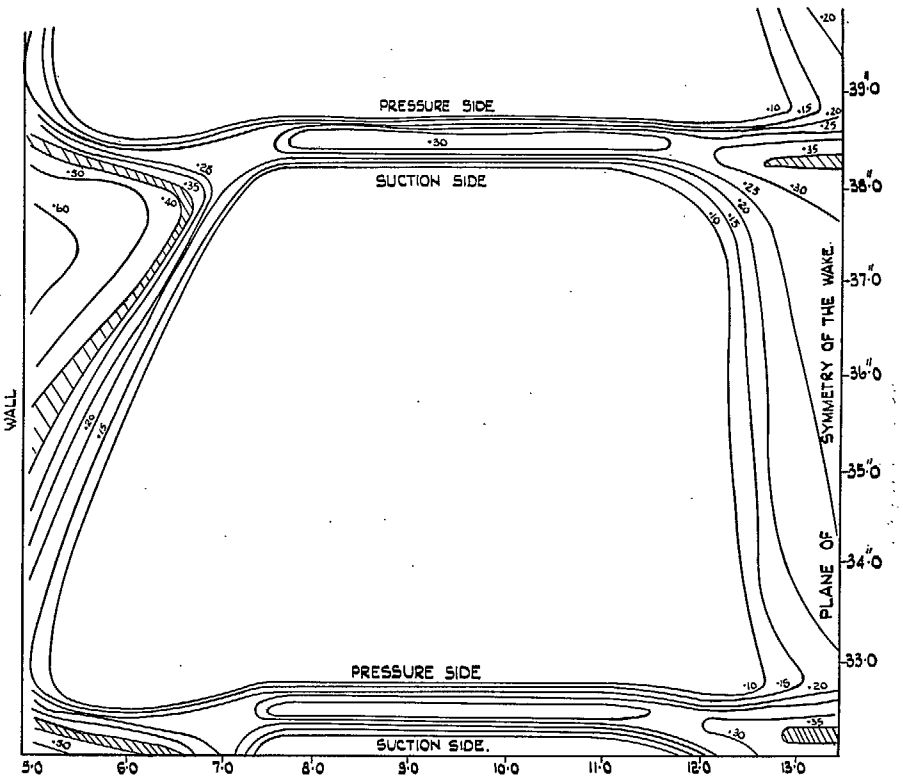

FIG. 2. Test I.—Total-head decrement contours 2 in. downstream of the cascade ($\alpha_1 = 55$ deg; $\theta = 30$ deg; $Re = 2{\cdot}5 \times 10^5$; static-pressure-rise coefficient $\Delta p/\frac{1}{2}\rho V^2 = 0{\cdot}333$).

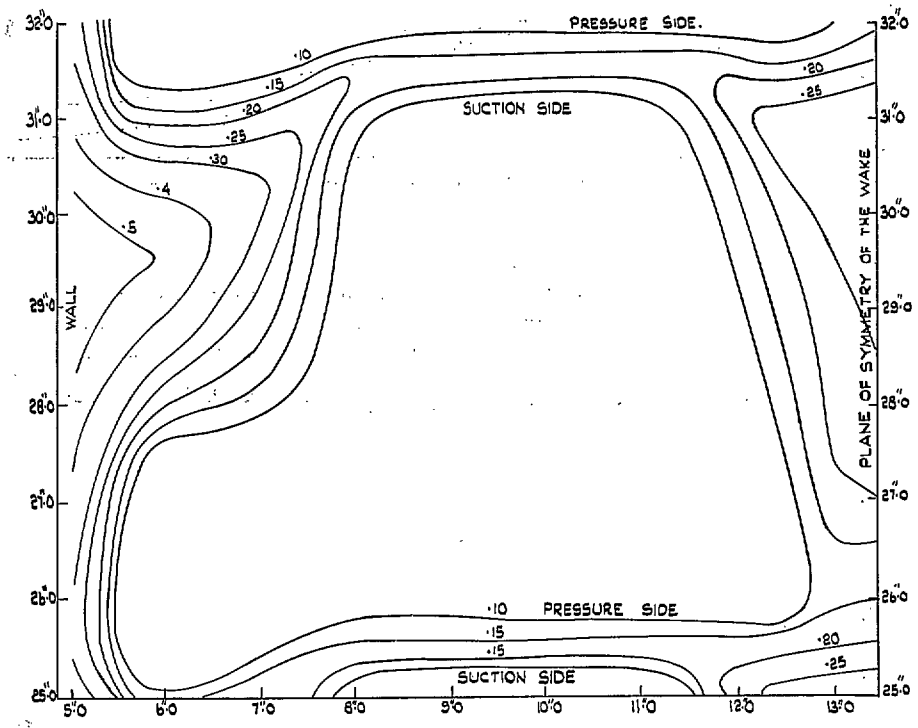

FIG. 3. Test Ib.—Total-head-decrement contours 6 in. downstream of the cascade ($\alpha_1 = 55$ deg; $\theta = 30$ deg; $Re = 2{\cdot}5 \times 10^5$; static-pressure-rise coefficient $\Delta p/\frac{1}{2}\rho V^2 = 0{\cdot}333$).

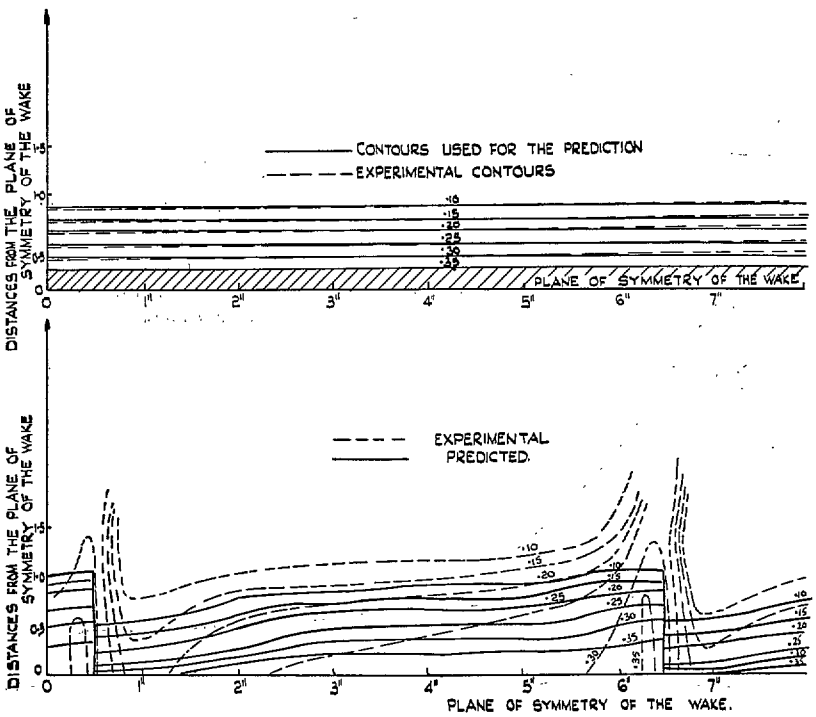

FIG. 4. Total-head-decrement contours upstream (Upper Figure).
Predicted and experimental contours downstream of the cascade (Lower Figure).

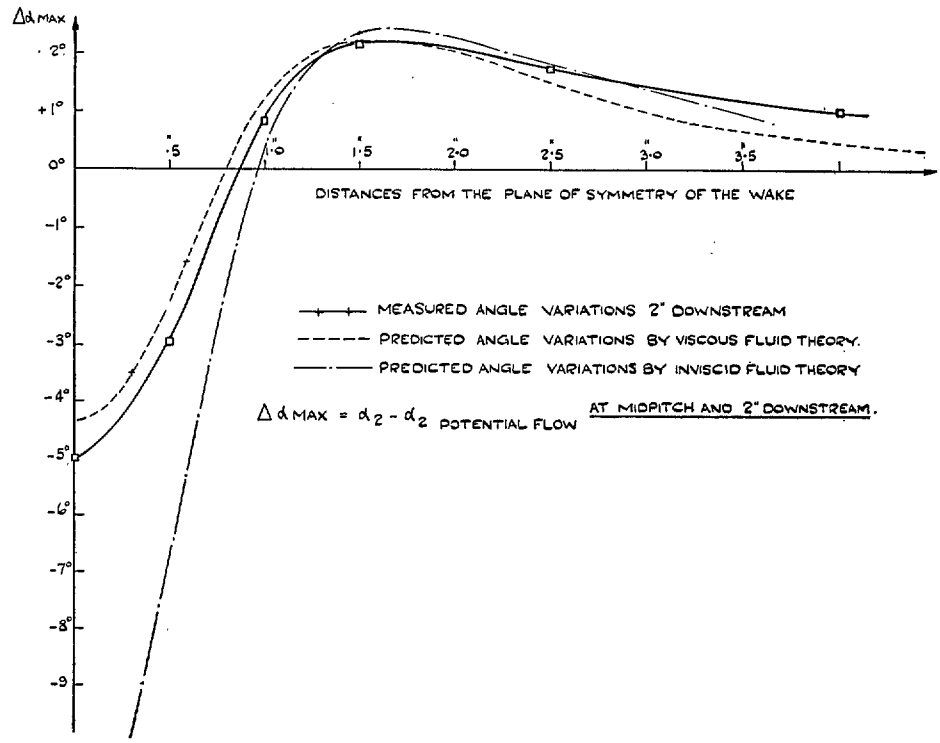

FIG. 5. Angle variations.

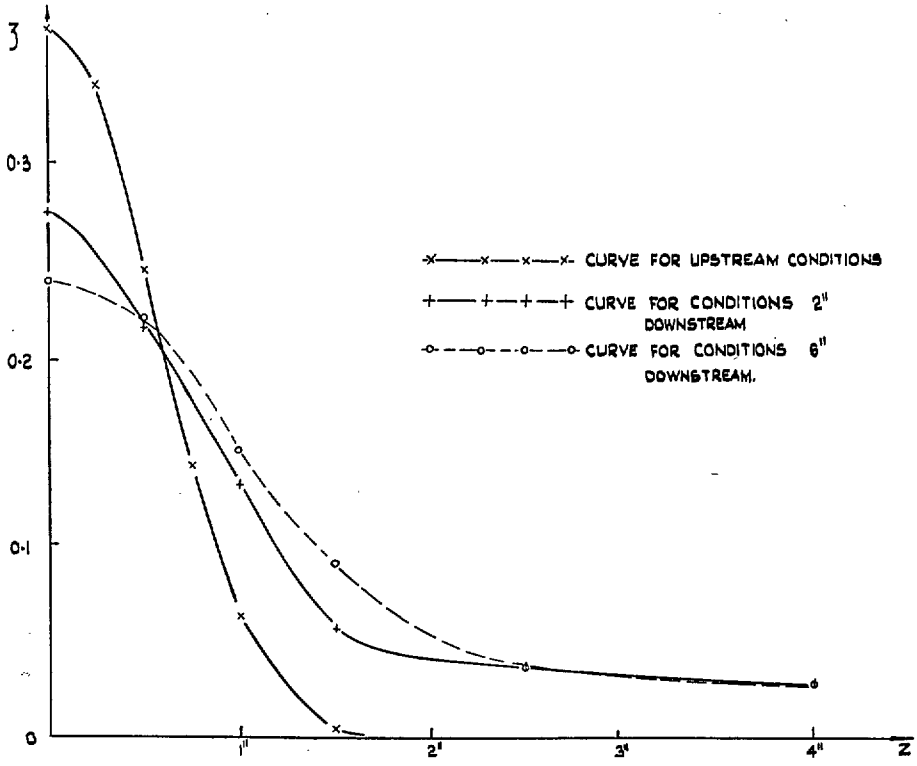

FIG. 6. Test I.—Averaged total-pressure-loss coefficient on a pitch length at different distances z from the plane of symmetry of the wake.

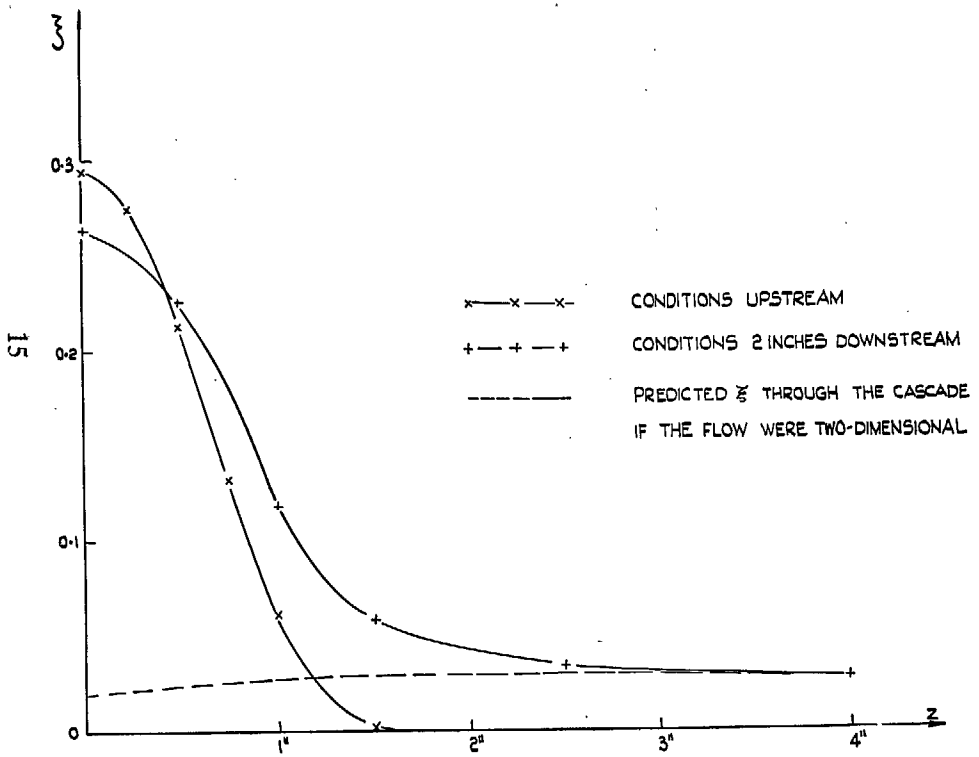

FIG. 7. Test I.—Mass-averaged total-pressure-loss coefficient on a pitch length at different distances z from the plane of symmetry of the wake.

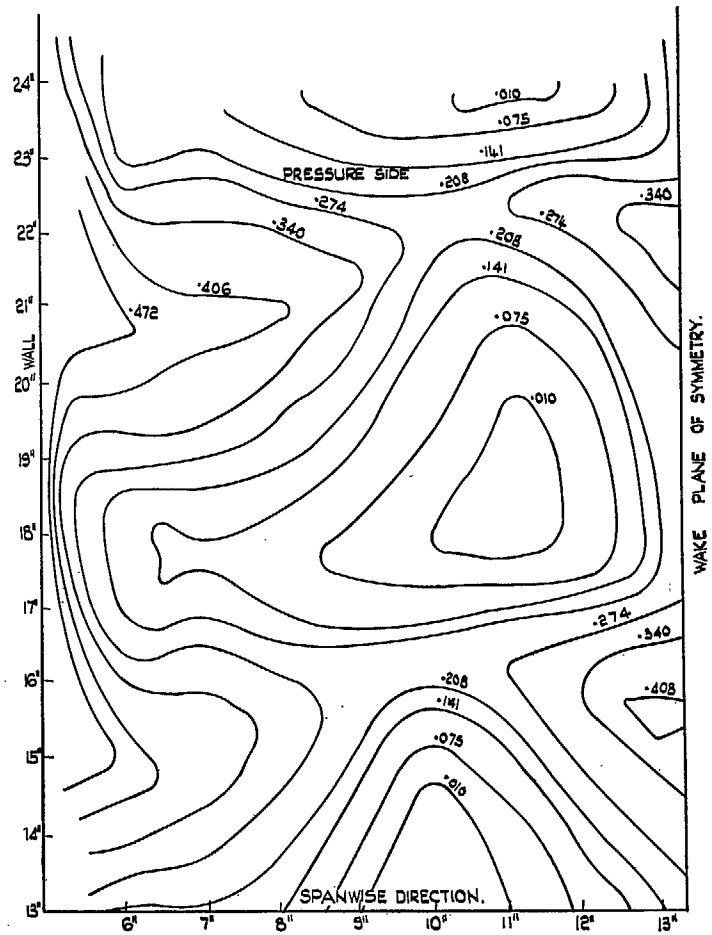

FIG. 8. Total-head decrement contours 6 in. downstream of the cascade.—Test II: $\alpha_1 = 63$ deg; $\theta = 30$ deg; $Re = 2{\cdot}5 \times 10^5$; static-pressure-rise coefficient $\Delta p/\frac{1}{2}\rho V^2 = 0{\cdot}278$.

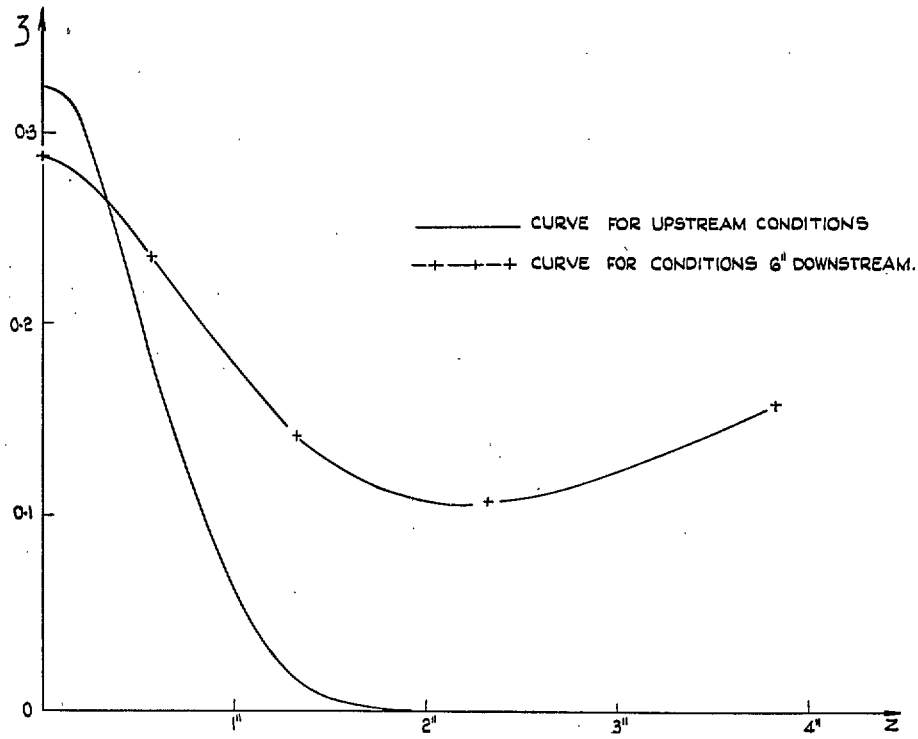

FIG. 9. Test II.—Mean total-pressure-loss coefficient over a pitch length at different distances z from the plane of symmetry of the wake.

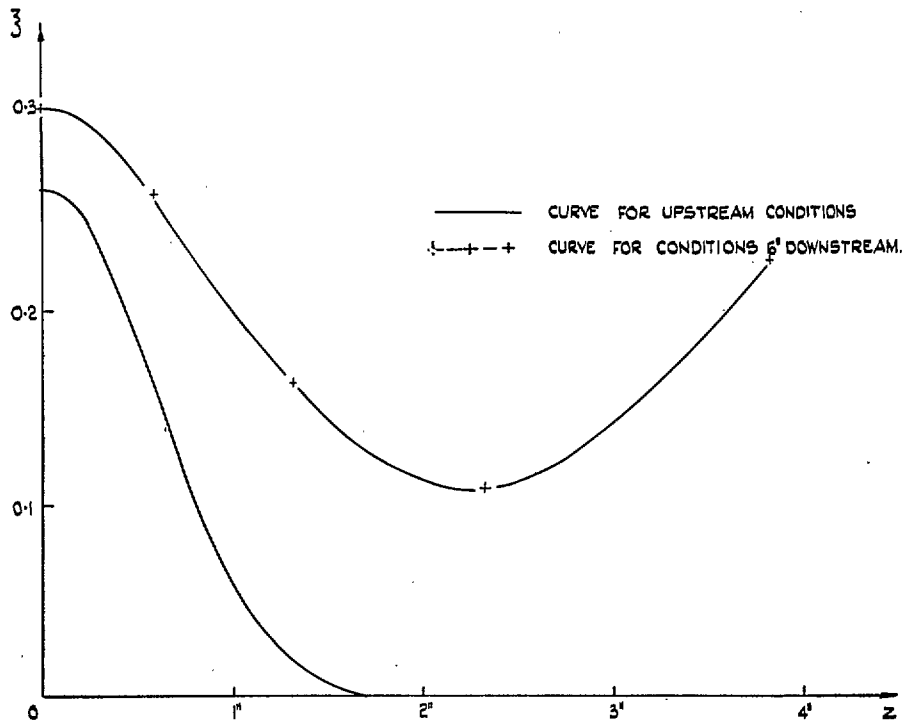

FIG. 10. Test II.—Mass-averaged pressure-loss coefficient over a pitch length at different distances z from the plane of symmetry of the wake.

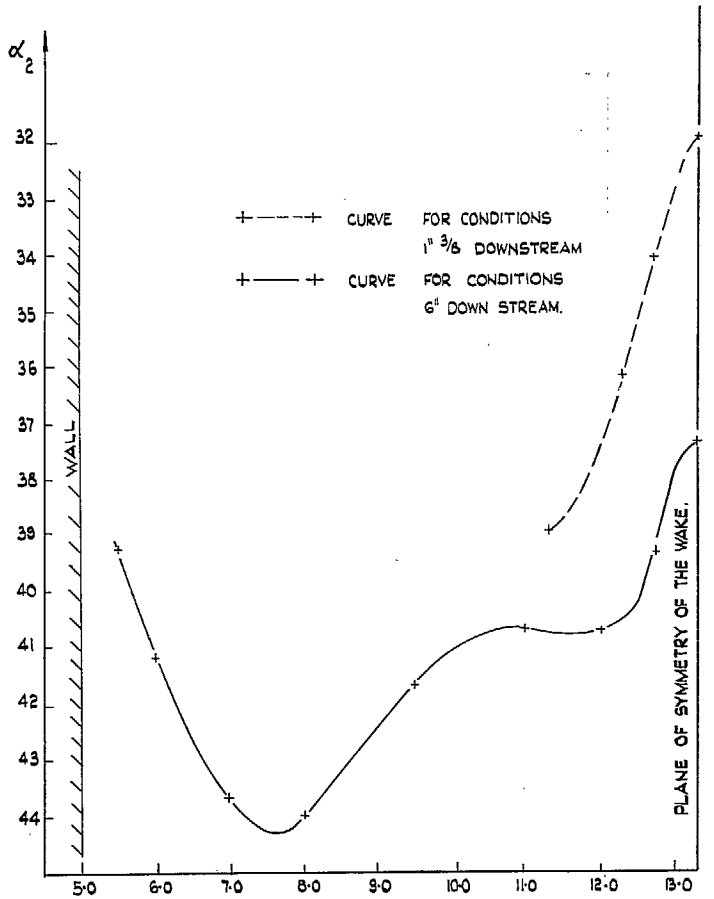

FIG. 11. Downstream outlet angles at mid-pitch.—Test II: Inlet air angle $\alpha_1 = 63° 05''$.

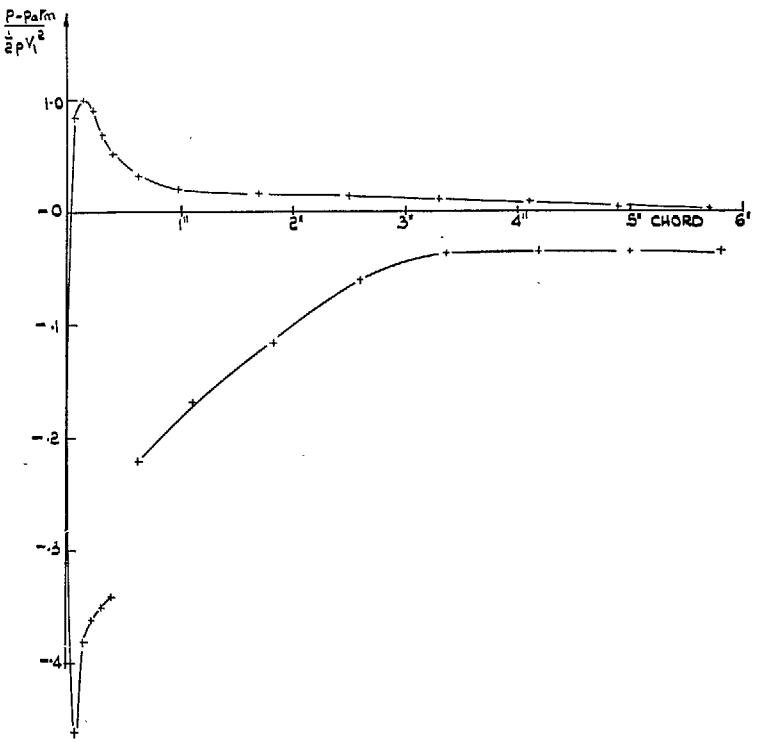

FIG. 12. Static-pressure distribution in the plane of symmetry of the cascade for an inlet angle $\alpha_1 = 63$ deg and an upstream uniform flow.

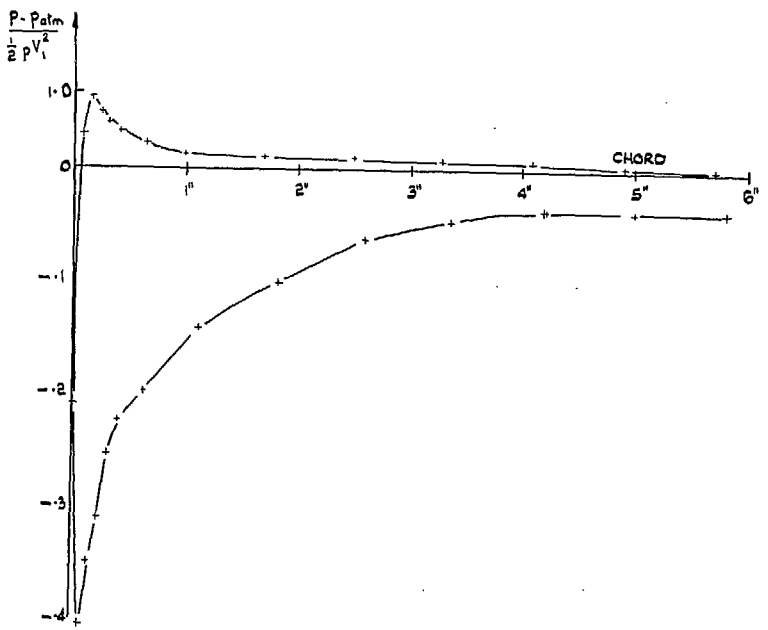

FIG. 13. Test II.—Static-pressure distribution in the plane of symmetry of the cascade.

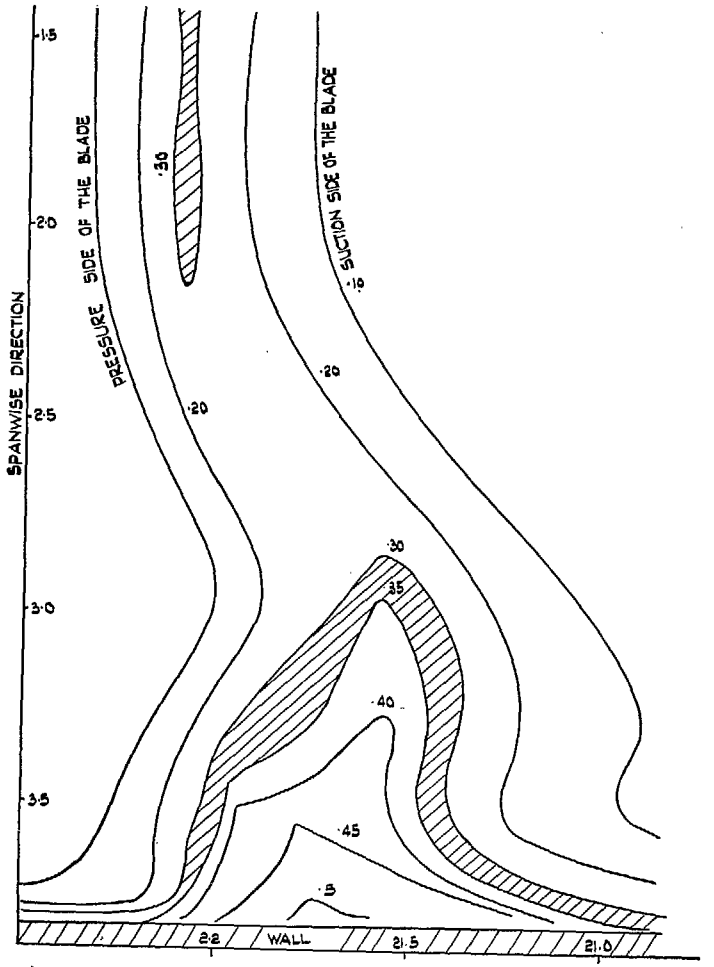

FIG. 14. Test IV.—Total-head-loss contours of the intersection of wall and blade ($Re = 2{\cdot}5 \times 10^5$).

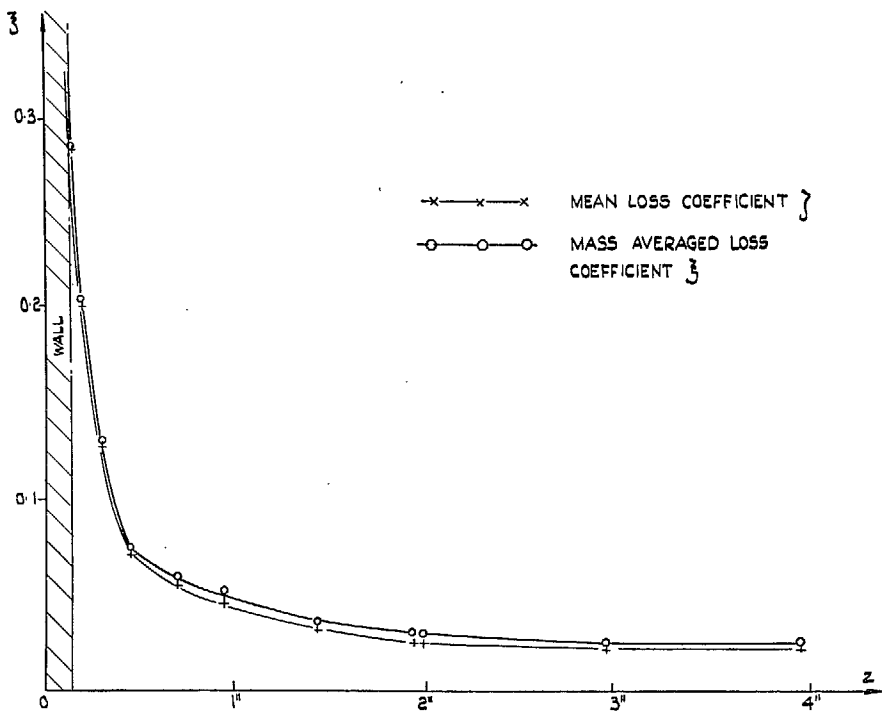

FIG. 15. Test IV.—Mean and mass-averaged loss coefficient over a pitch at different distances z from the mid-span plane.

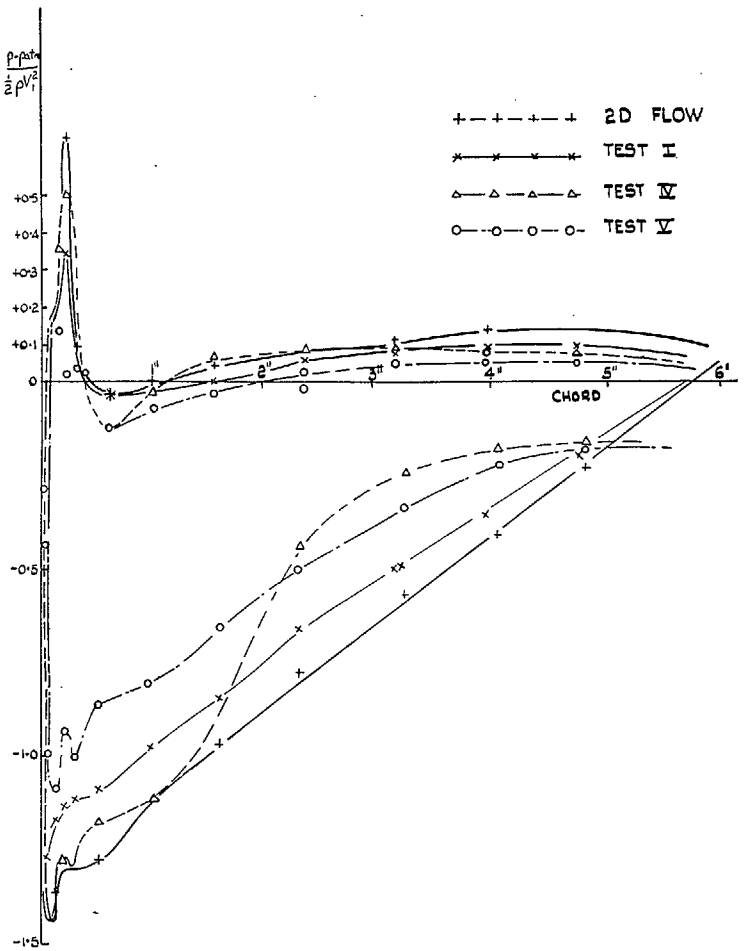

FIG. 16. Static-pressure distribution around a blade taken in the longitudinal plane of symmetry of the cascade.

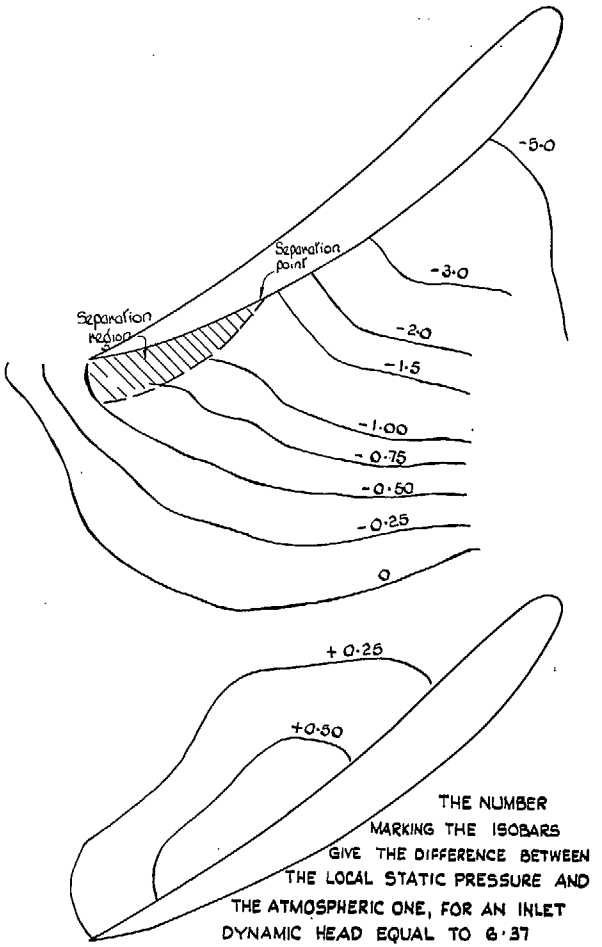

FIG. 17. Test IV.—Static-pressure distribution within a passage on the central wall. Evidence of a separation region.

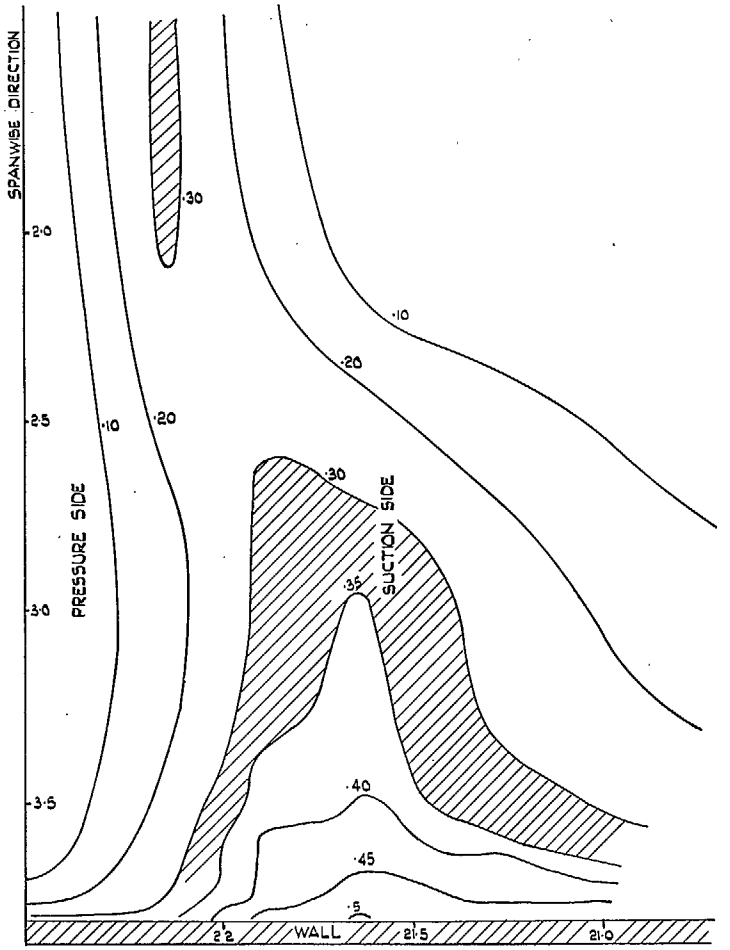

FIG. 18. Map of equal loss in total head lines ($\Delta p/\frac{1}{2}\rho V_1^2$); $Re = 2{\cdot}5 \times 10^5$; wall and wake: Test V.

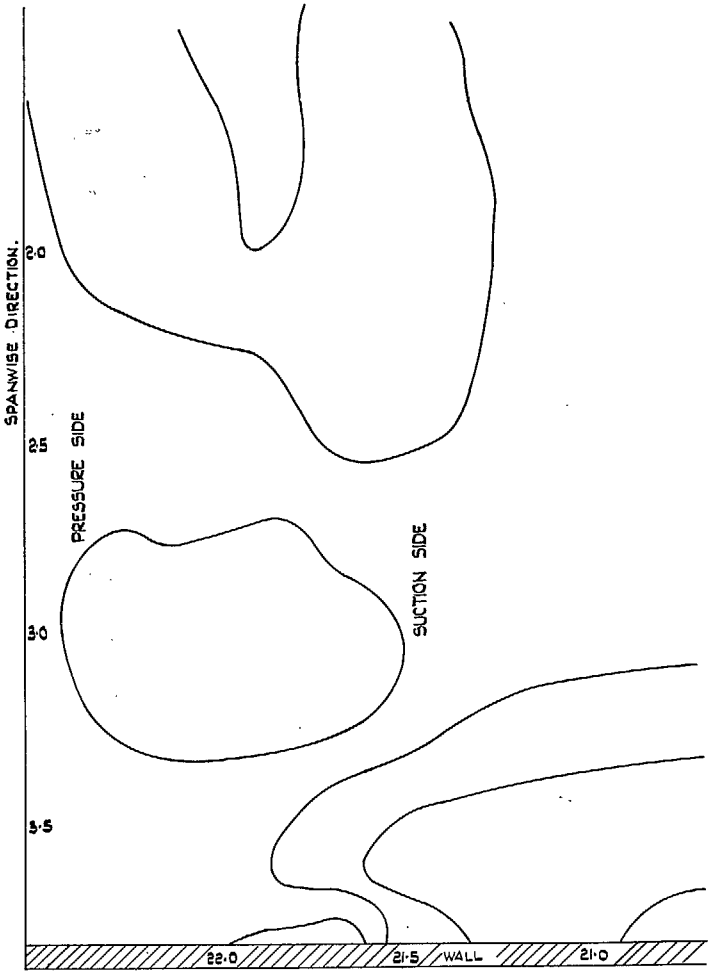

FIG. 19. Angle variations; $Re = 2{\cdot}5 \times 10^5$; wall and wake: Test V.

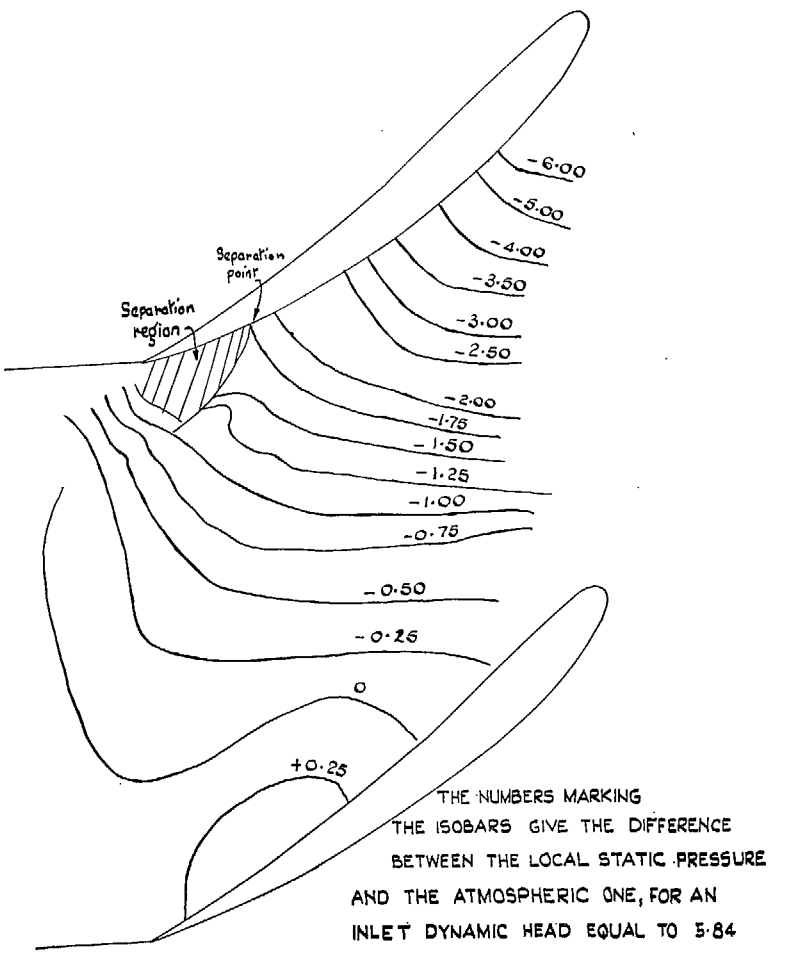

FIG. 20. Test V.—Static-pressure distribution within the passage on the central wall. Evidence of a separation region.

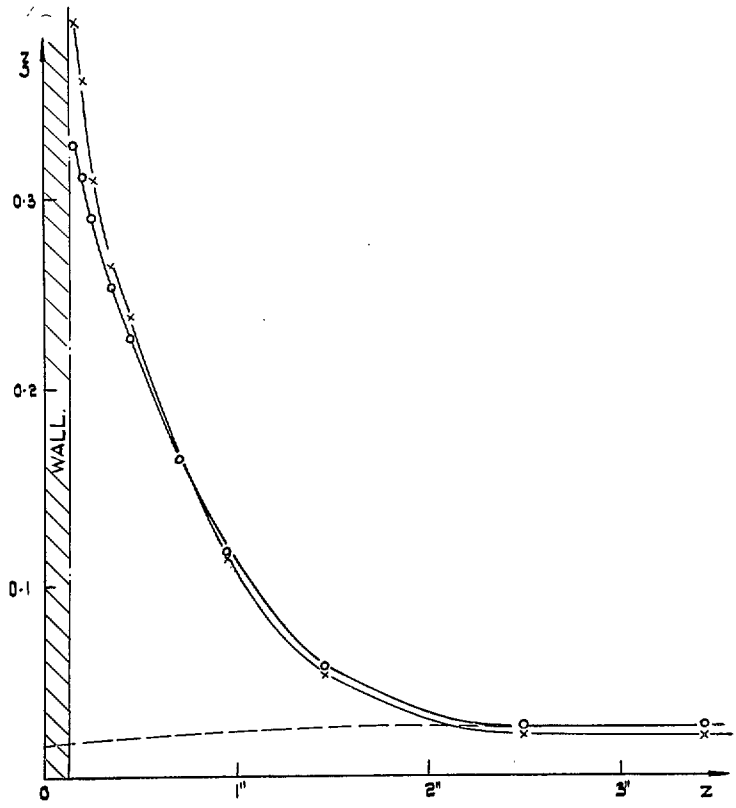

FIG. 21. Test V.—Mean and mass-averaged total-pressure-loss coefficient over a pitch length at different distances z from the plane of symmetry of the wake.

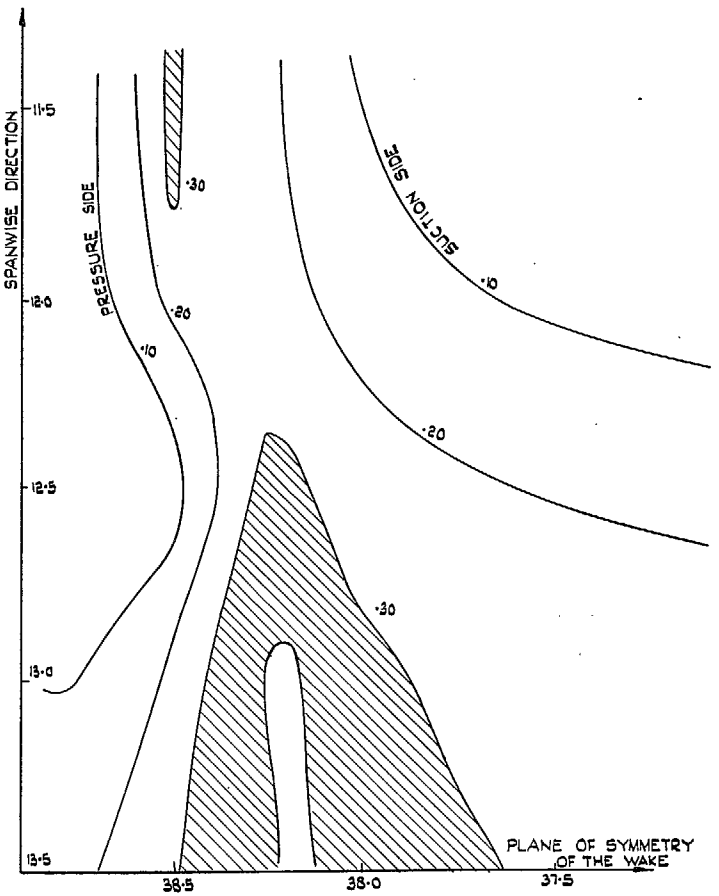

FIG. 22. Test I.—Total-head decrement contours downstream the cascade in the region around the intersection of a blade and the plane of symmetry of the wake.

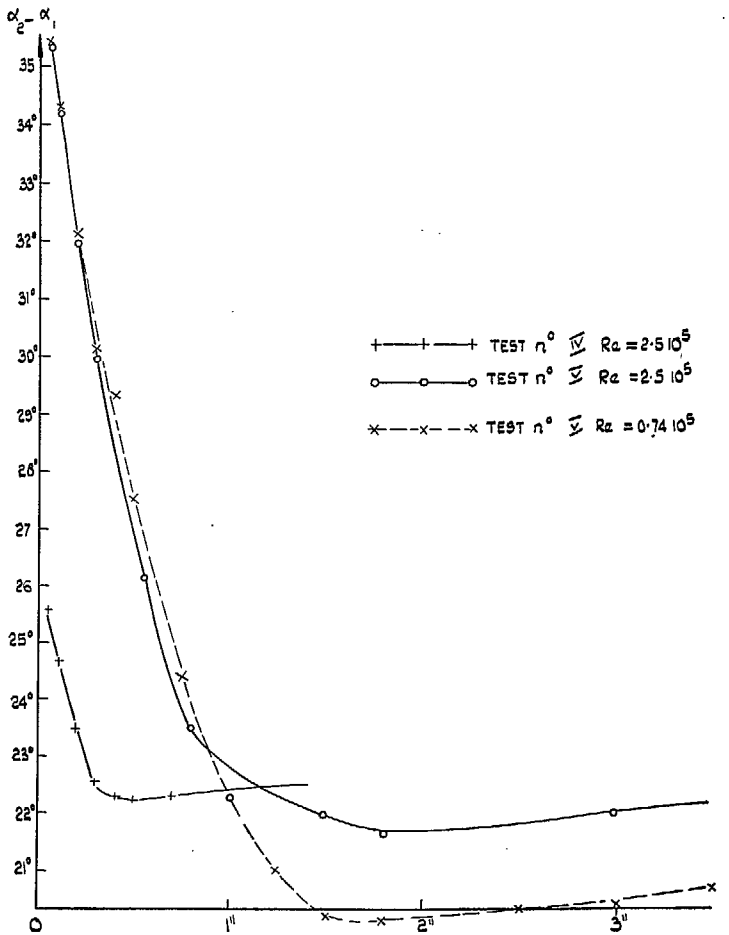

FIG. 23. Air deflection through the cascade at mid-pitch at different distances z from the wall.

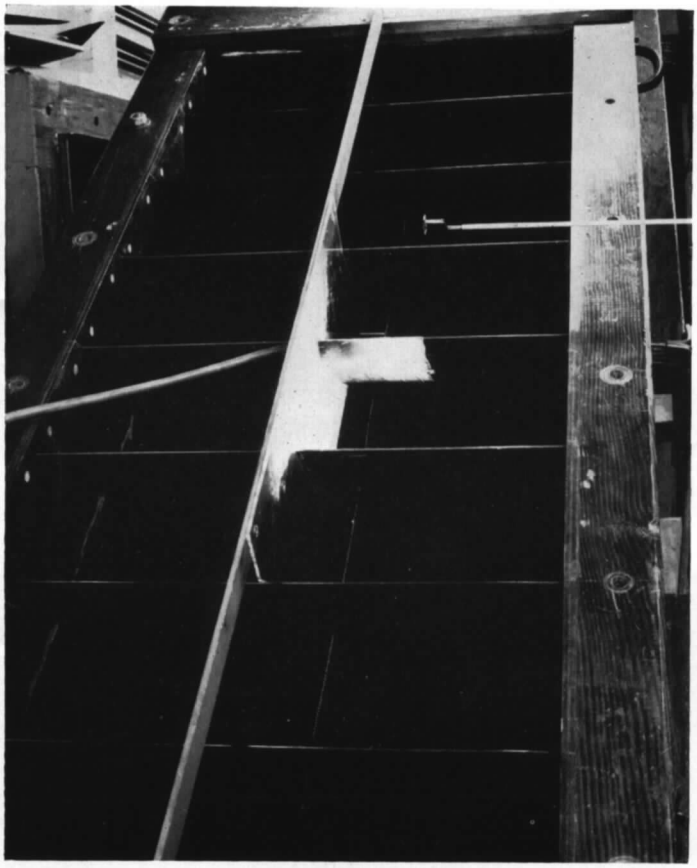

PHOTO. 1. General set-up for Experiment V.

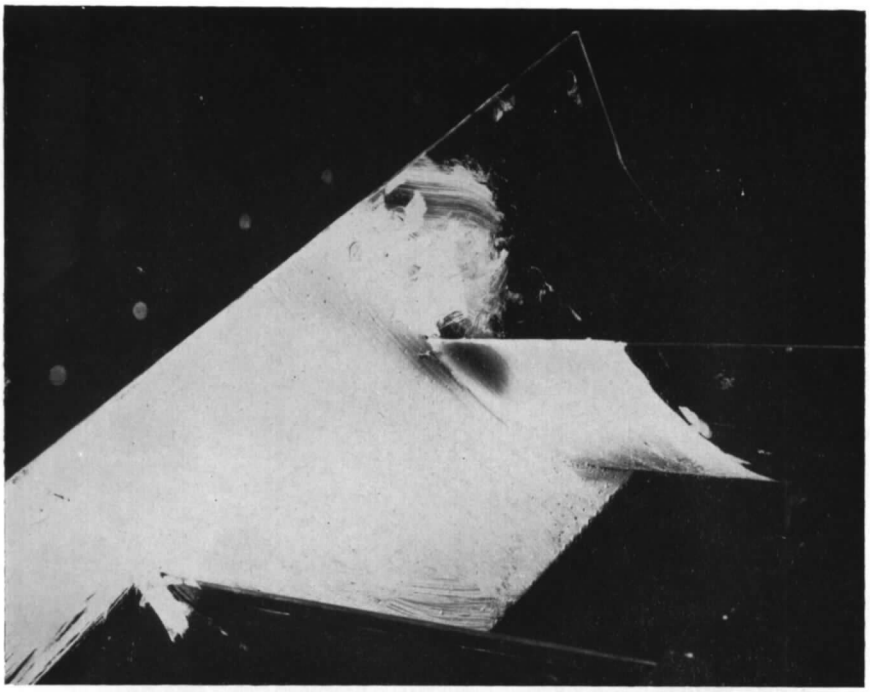

PHOTO. 2. ($Re = 2{\cdot}5 \times 10^5$).

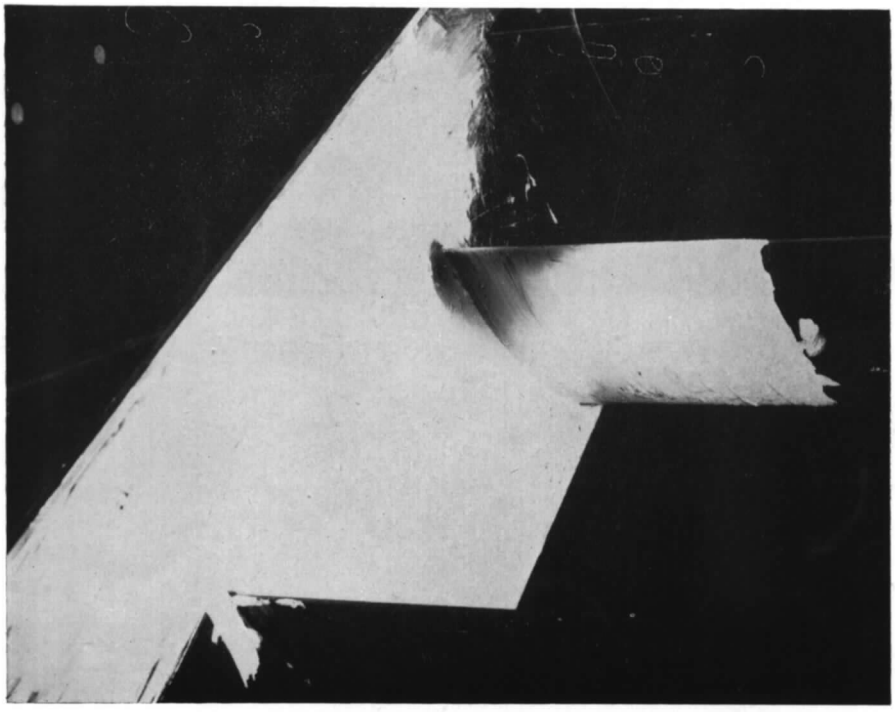

PHOTO. 3. ($Re = 0{\cdot}7 \times 10^5$).

PHOTOS. 2 and 3. Test IV.—Hydrogen-sulphide traces in a blade channel.

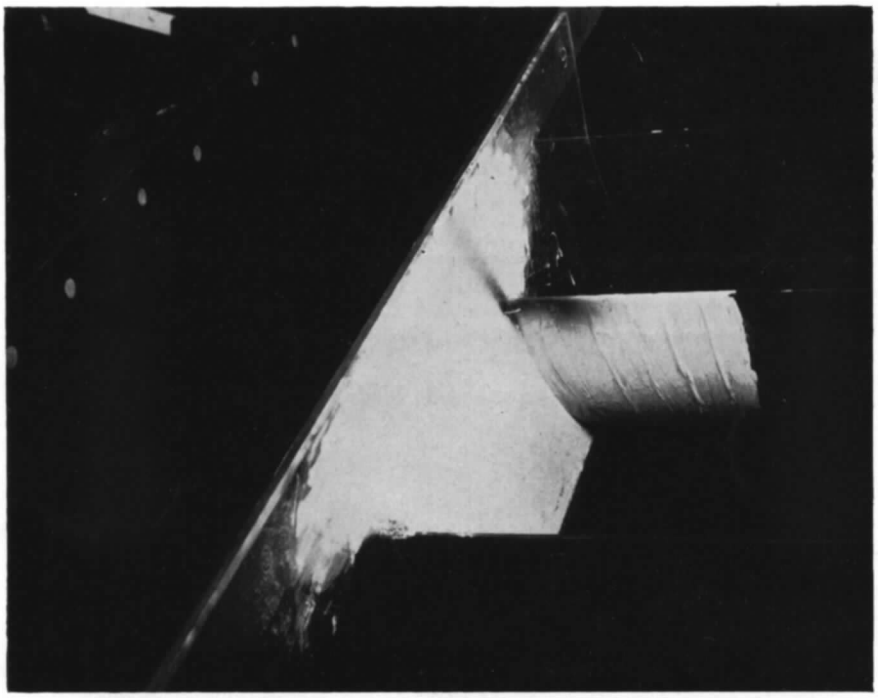

PHOTO. 4. ($Re = 2{\cdot}5 \times 10^5$).

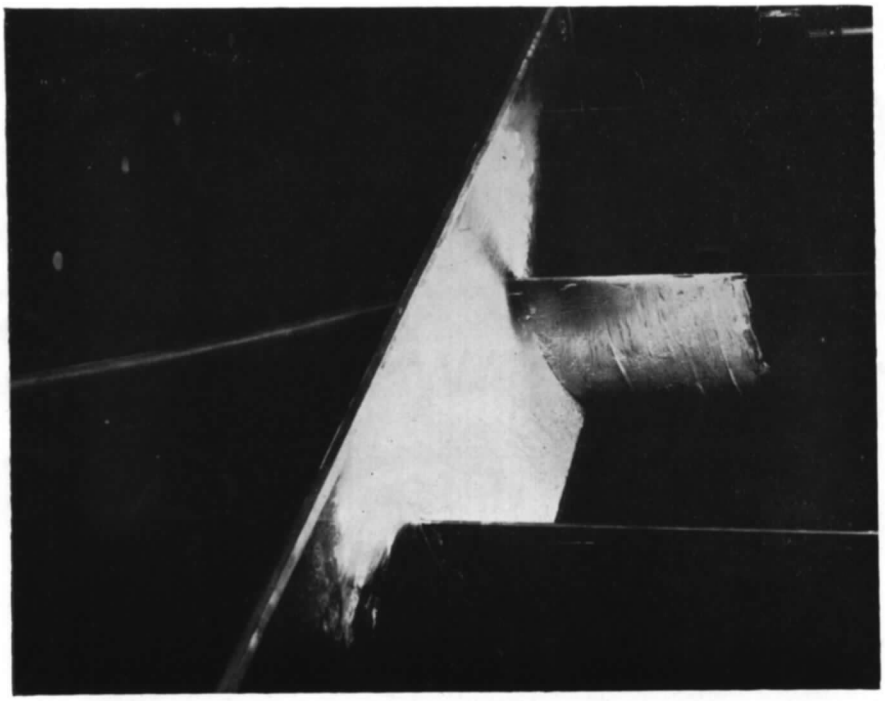

PHOTO. 5. ($Re = 0{\cdot}7 \times 10^5$).

PHOTOS. 4 and 5. Test V.—Hydrogen-sulphide traces in a blade channel.

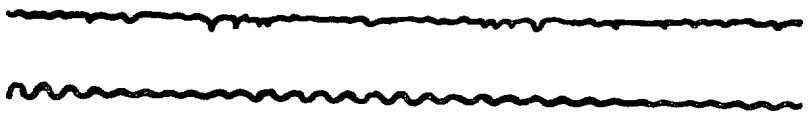

PHOTO. 6. Turbulence in the wake of a blade immersed in the main flow.

PHOTO. 7. Turbulence close to the wall at mid-pitch position.

PHOTO. 8. Large-scale turbulence due to corner stall.

(78797) Wt. 54/8210 K.5 9/60 Hw.

Publications of the Aeronautical Research Council

ANNUAL TECHNICAL REPORTS OF THE AERONAUTICAL RESEARCH COUNCIL (BOUND VOLUMES)

1941 Aero and Hydrodynamics, Aerofoils, Airscrews, Engines, Flutter, Stability and Control, Structures. 63*s.* (post 2*s.* 3*d.*)

1942 Vol. I. Aero and Hydrodynamics, Aerofoils, Airscrews, Engines. 75*s.* (post 2*s.* 3*d.*)
Vol. II. Noise, Parachutes, Stability and Control, Structures, Vibration, Wind Tunnels. 47*s.* 6*d.* (post 1*s.* 9*d.*)

1943 Vol. I. Aerodynamics, Aerofoils, Airscrews. 80*s.* (post 2*s.*)
Vol. II. Engines, Flutter, Materials, Parachutes, Performance, Stability and Control, Structures. 90*s.* (post 2*s.* 3*d.*)

1944 Vol. I. Aero and Hydrodynamics, Aerofoils, Aircraft, Airscrews, Controls. 84*s.* (post 2*s.* 6*d.*)
Vol. II. Flutter and Vibration, Materials, Miscellaneous, Navigation, Parachutes, Performance, Plates and Panels, Stability, Structures, Test Equipment, Wind Tunnels. 84*s.* (post 2*s.* 6*d.*)

1945 Vol. I. Aero and Hydrodynamics, Aerofoils. 130*s.* (post 2*s.* 9*d.*)
Vol. II. Aircraft, Airscrews, Controls. 130*s.* (post 2*s.* 9*d.*)
Vol. III. Flutter and Vibration, Instruments, Miscellaneous, Parachutes, Plates and Panels, Propulsion. 130*s.* (post 2*s.* 6*d.*)
Vol. IV. Stability, Structures, Wind Tunnels, Wind Tunnel Technique. 130*s.* (post 2*s.* 6*d.*)

Special Volumes

Vol. I. Aero and Hydrodynamics, Aerofoils, Controls, Flutter, Kites, Parachutes, Performance, Propulsion, Stability. 126*s.* (post 2*s.* 6*d.*)

Vol. II. Aero and Hydrodynamics, Aerofoils, Airscrews, Controls, Flutter, Materials, Miscellaneous, Parachutes, Propulsion, Stability, Structures. 147*s.* (post 2*s.* 6*d.*)

Vol. III. Aero and Hydrodynamics, Aerofoils, Airscrews, Controls, Flutter, Kites, Miscellaneous, Parachutes, Propulsion, Seaplanes, Stability, Structures, Test Equipment. 189*s.* (post 3*s.* 3*d.*)

Reviews of the Aeronautical Research Council

1939–48 3*s.* (post 5*d.*) 1949–54 5*s.* (post 6*d.*)

Index to all Reports and Memoranda published in the Annual Technical Reports

1909–1947 R. & M. 2600 6*s.* (post 4*d.*)

Author Index to the Reports and Memoranda and Current Papers of the Aeronautical Research Council

February, 1954–February, 1958 R. & M. No. 2570 (Revised) (Addendum) 7*s.* 6*d.* (post 4*d.*)

Indexes to the Technical Reports of the Aeronautical Research Council

July 1, 1946–December 31, 1946 R. & M. No. 2150 1*s.* 3*d.* (post 2*d.*)

Published Reports and Memoranda of the Aeronautical Research Council

Between Nos. 2251–2349	R. & M. No. 2350 1*s.* 9*d.* (post 2*d.*)
Between Nos. 2351–2449	R. & M. No. 2450 2*s.* (post 2*d.*)
Between Nos. 2451–2549	R. & M. No. 2550 2*s.* 6*d.* (post 2*d.*)
Between Nos. 2551–2649	R. & M. No. 2650 2*s.* 6*d.* (post 2*d.*)
Between Nos. 2651–2749	R. & M. No. 2750 2*s.* 6*d.* (post 2*d.*)
Between Nos. 2751–2849	R. & M. No. 2850 2*s.* 6*d.* (post 2*d.*)
Between Nos. 2851–2949	R. & M. No. 2950 3*s.* (post 2*d.*)

HER MAJESTY'S STATIONERY OFFICE

from the addresses overleaf

Printed and published by
HER MAJESTY'S STATIONERY OFFICE

To be purchased from
York House, Kingsway, London W.C.2
423 Oxford Street, London W.1
13A Castle Street, Edinburgh 2
109 St. Mary Street, Cardiff
39 King Street, Manchester 2
50 Fairfax Street, Bristol 1
2 Edmund Street, Birmingham 3
80 Chichester Street, Belfast 1
or through any bookseller

Printed in England

R. & M. No. 3136

S.O. Code No. 23-3136